Published in final edited form as:
Nature. 2007 July 12; 448(7150): 200–203. doi:10.1038/nature05926.

An intracellular P2X receptor required for osmoregulation in *Dictyostelium discoideum*

Samuel J. Fountain[1], **Katie Parkinson**[1], **Mark T. Young**[1], **Lishuang Cao**[1], **Christopher R. L. Thompson**[1], and **R. Alan North**[1]

[1]Faculty of Life Sciences, University of Manchester, Michael Smith Building, Oxford Road, Manchester M13 9PT, UK.

Abstract

P2X receptors are membrane ion channels gated by extracellular ATP1,2 that are found widely in vertebrates, but not previously in microbes. Here we identify a weakly related gene in the genome of the social amoeba *Dictyostelium discoideum*, and show, with the use of heterologous expression in human embryonic kidney cells, that it encodes a membrane ion channel activated by ATP (30–100 μM). Site-directed mutagenesis revealed essential conservation of structure–function relations with P2X receptors of higher organisms. The receptor was insensitive to the usual P2X antagonists3 but was blocked by nanomolar concentrations of Cu^{2+} ions. In *D. discoideum*, the receptor was found on intracellular membranes, with prominent localization to an osmoregulatory organelle, the contractile vacuole. Targeted disruption of the gene in *D. discoideum* resulted in cells that were unable to regulate cell volume in hypotonic conditions. Cell swelling in these mutant cells was accompanied by a marked inhibition of contractile vacuole emptying. These findings demonstrate a new functional role for P2X receptors on intracellular organelles, in this case in osmoregulation.

The *D. discoideum* genome contains five sequences predicted to encode proteins homologous to vertebrate P2X receptors. The protein most closely related to the seven human receptors is DDB0168616 (Supplementary Fig. 1). HEK cells expressing a humanized version of this complementary DNA responded to ATP with robust inward currents (Fig. 1). ATP evoked unitary currents (conductance 8.2 pS at –100 mV) in outside-out patches (Fig. 1a, b), establishing that this gene (*D. discoideum p2xA*) encodes an ATP-gated ion channel (*Dd*P2X). Whole-cell currents evoked by ATP were concentration-dependent (10–300 μM) with kinetic properties most similar to those observed for human $P2X_2$ or $P2X_4$ receptors1 (Fig. 1d). With sodium as the only cation, the current–voltage relation reversed at zero and showed moderate inward rectification (Fig. 1c). By measuring the current reversal potentials in different extracellular ions, we found that the channels were freely permeable to Ca^{2+} ions but less so to larger cations (the relative permeability P_X/P_{Na} was 1.5 ± 0.11 (n = 8 cells), 0.54 ± 0.01 (5), 0.48 ± 0.21 (5), 0.38 ± 0.16 (5) and 0.21 ± 0.05 (8), where X represents Ca^{2+}, choline, Tris, tetraethylammonium and *N*-methyl-D-glucamine, respectively; Fig. 1c). These values are in the range of vertebrate P2X receptors1. Western blotting of the expressed receptor showed two bands at 48 and 55 kDa (Fig. 1e). The

Correspondence and requests for materials should be addressed to C.R.L.T. (christopher.thompson@manchester.ac.uk) or R.A.N. (r.a.north@manchester.ac.uk)..

Supplementary Information is linked to the online version of the paper at www.nature.com/nature.

The authors declare no competing financial interests.

Europe PMC Funders Author Manuscripts

receptor formed a trimer under non-denaturing conditions (Fig. 1e), and immunocytochemistry indicated that the expressed receptor was clearly localized at the plasma membrane (Fig. 1f). These data are consistent with a body of evidence indicating that vertebrate P2X receptors are trimeric membrane proteins1,2,4,5.

The *Dd*P2X receptor was strongly activated by hydrolysis-resistant ATP analogues. βγ-Imido-ATP was about tenfold more potent than ATP, and αβ-methylene-ATP was equipotent with ATP (Fig. 2a, b). The receptor was only weakly activated by 2′,3′-*O*-(4-benzoylbenzoyl)-ATP, and not at all by UTP, CTP, GTP, ADP, cyclic AMP, NAD^+, FAD, ADP-ribose and cyclic ADP-ribose (1 mM). Most P2X receptors are blocked by suramin and pyridoxal-phosphate-6-azophenyl-2′,4′-disulphonate, whereas $P2X_1$, $P2X_3$ and $P2X_{2/3}$ heteromeric receptors are blocked by nanomolar concentrations of 2′,3′-*O*-(2,4,6-trinitrophenyl)-ATP1,3: none of these antagonists inhibited the currents at *Dd*P2X receptors, even at 30–100 μM (Fig. 2c). However, *Dd*P2X was very sensitive to block by Cu^{2+} (half-maximal inhibitory concentration(IC_{50}) 40 ± 5 nM, *n* = 5; Fig.2c), whereas other divalent ions were much less effective (Ni^{2+} IC_{50} 59 ± 5 μM; Ca^{2+} IC_{50} >20 mM; *n* = 5). Inhibition by micromolar Cu^{2+} has been described for some ($P2X_4$, $P2X_7$) but not other mammalian P2X receptors6,7.

We tested the essential similarity in molecular physiology between the *Dd*P2X receptor and its vertebrate counterparts by mutating residues known to be critically involved in function1,8,9. A body of work implicates two lysine residues in the receptor ectodomain as contributing to ATP binding. The first of these (*Dd*P2X Lys 67) is in a position equivalent to Lys 71 of the rat $P2X_2$ receptor (Supplementary Fig. 1); mutation to alanine (*Dd*P2X[K67A]) caused a large (more than tenfold) decrease in ATP sensitivity. The second, *Dd*P2X Lys 289, aligns with rat $P2X_2$ receptor Lys 308; ATP elicited much smaller currents at *Dd*P2X[K289A] (Fig. 2d, e). An aspartate residue in the second transmembrane domain is essential for function in vertebrate P2X receptors1; the *Dictyostelium* receptor in which this was replaced by alanine [D330A] was also non-functional. Finally, a YXXXK motif at the carboxy terminus of all vertebrate P2X receptors is involved in receptor stabilization at the plasma membrane10; this motif was also required in *Dd*P2X for robust membrane currents (Fig. 2d). Conversely, some regions of the receptor that have been deduced to be critical for ATP binding and/or channel activation in mammalian P2X receptors were clearly not essential. These included the conserved NFTΦΦΦKNSΦ (Φ being any hydrophobic residue) and GYNFRFAKY motifs in the ectodomain of mammalian receptors. The former motif is found in *Dd*P2X (SFTILIDHTM), but in contrast with the human $P2X_1$ receptor9 the phenylalanine residue (Phe 156) was not required for ATP action (Fig. 2d, e). The latter motif is not present in the *Dd*P2X sequence.

A green fluorescent protein (GFP)-tagged version of *Dd*P2X (*Dd*P2X–GFP) was localized to intracellular membranes of *D. discoideum* cells rather than the plasma membrane (Fig. 3a), contrary to what is observed either for P2X receptors in mammalian cells or for *Dd*P2X receptors expressed in HEK 293 cells (Fig. 1f). Strong co-localization with calmodulin demonstrated prominent expression on the membrane of the contractile vacuole (Fig. 3a), a specialized osmoregulatory organelle that allows protists to survive in hypotonic environments such as soil and fresh water11-14. Identification of *Dd*P2X as a contractile vacuole protein thus indicated that *Dd*P2X receptors might be involved in osmoregulation. To test this, we generated mutant cells with a disrupted *p2xA* gene by homologous recombination (Fig. 3b) and assayed for osmoregulatory defects. In hypotonic conditions, wild-type cells swelled by about 20%, followed by a regulatory decrease in cell volume over the next 40 min (Fig. 3c, d; *n* = 30 cells). In contrast, *Dd*P2X-null cells showed no regulatory decrease in cell volume but continued to swell over 60 min (Fig. 3; *n* = 30 cells, $P<0.01$). Two lines of evidence indicate that this phenotype is due to a requirement for

*Dd*P2X receptors in wild-type cells. First, expression of *Dd*P2X–GFP in the *Dd*P2X-null cells rescued the osmoregulatory defects of the mutant (Fig. 3d). Second, Cu^{2+} at concentrations that blocked *Dd*P2X currents when expressed in HEK 293 cells (Fig. 2) recapitulated the swelling phenotype in wild-type cells (Fig. 3d). Furthermore, βγ-imido-ATP (100 μM), which is polar and cell-impermeant, had no effect on the regulatory decrease in volume when applied to wild-type cells; this discounts a role for plasma membrane receptors and is consistent with the intracellular compartmentalization of *Dd*P2X. Taken together, these data indicate a direct role for *Dd*P2X receptors in osmoregulation.

In wild-type cells, the contractile vacuole periodically fills and voids, expelling water from the cell body and permitting the regulatory decrease in volume under hypotonic conditions. We therefore tested whether an impairment of contractile vacuole function could explain why *Dd*P2X-disrupted cells displayed no regulatory decrease in volume. In wild-type cells, regular voiding events occurred with a cycle of 80 ± 5s(n = 30 cells; Fig. 3e). In contrast, mutant cells had a decreased frequency of contractile vacuole voiding and a prolonged cycle (182 ± 10 s, n = 30 cells; Fig. 3e). Wild-type cells treated with 10 μM Cu^{2+} also had a prolonged voiding cycle (202 ± 13 s, n = 15 cells). These results suggest that loss of the *Dd*P2X receptor leads to a compromised contractile vacuole, an inability to osmoregulate, and ultimately cell swelling. Contractile vacuole filling seemed to be normal in *Dd*P2X-null cells, implying that docking at the cell membrane or the contraction itself is deficient. It is possible that the Ca^{2+} permeability of the P2X receptor in the membrane of the contractile vacuole has a key function. In concord with this idea, the pheno-type of *Dd*P2X-disrupted cells is similar to that of LvsA-null cells, which is thought to be partly due to a misregulation of calmodulin function15,16. One speculative possibility is that distension of the contractile vacuole leads to the entry of ATP from the cell cytoplasm: this then activates *Dd*P2X receptors, which allow vacuolar Ca^{2+} ions to pass back into the cytoplasm and initiate contraction.

These studies represent significant advances for the study of P2X receptor structure and function. The *Dd*P2X receptor reported here is relatively remote in sequence from those previously reported1,17. Despite this, essential properties of a P2X receptor (ATP binding, channel gating and permeation) are conserved between amoeba and man. Consequently, attention can now be drawn to those few parts of the molecule critical to these functions. P2X receptors have hitherto been considered in the context of the plasma membrane and the transmitter-like actions of extracellular ATP1,2. The present studies, however, define a receptor that is both found on internal membranes and has an intracellular role. This raises the possibility that P2X receptors might also function as intracellular ion channels in other cell types, including higher organisms. Such an idea is not without precedent. Another family of channel proteins (ClC chloride channels) has members with well-defined functional roles in both plasma and endosomal membranes17. Furthermore, some members of the family of ‘ectoenzyme’ nucleoside triphosphate diphosphohydrolases are actually found predominantly on internal membranes18. Given the ubiquitous presence of their ligand ATP, P2X receptors may be more general regulators of intracellular organelles in ways other than osmoregulation.

METHODS

Generation and expression of *Dd*P2X constructs

A 1.1-kilobase cDNA corresponding to the predicted open reading frame of DDB0168616 was amplified by polymerase chain reaction from growth-phase AX4 strain *D. discoideum*. The insert was subcloned into pcDNA3.1-His at 5′ *Bam*HI and 3′ *Xho*I sites and into pDEX 27 GFP at *Eco*RI sites for expression in HEK 293 cells and *D. discoideum*, respectively. Expression of the pcDNA3.1 *Dd*P2X construct in HEK 293 cells produced messenger RNA

transcript but no detectable protein or function. A humanized version of the *Dd*P2X receptor was synthesized in which each amino acid codon was replaced by that most commonly found in *Homo sapiens*. This was C-terminally tagged with hexahistidine (DNA 2.0 Inc.) and subcloned into pcDNA3.1. For electrophysiology, HEK 293 cells were transiently transfected with 1 μg (whole-cell) or 0.1 μg (outside-out) plus 0.1 μg of enhanced GFP using Lipofectamine 2000. For expression in *D. discoideum*, cells were transformed by electroporation and subjected to G418 selection.

Electrophysiology

Whole-cell and outside-out patch recordings were made from HEK 293 cells at room temperature (18–20 °C), 24–48 h after transient transfection. The extracellular solution contained (in mM): 145 NaCl, 2 KCl, 2 $CaCl_2$, 1 $MgCl_2$,13 D-glucose and 10 HEPES, pH 7.3. For whole-cell recordings, the intracellular patch pipette solution contained (in mM): 145 NaCl, 10 HEPES and 10 EGTA, pH 7.3. For outside-out recordings, NaF replaced NaCl in the patch pipette. Outside-out recordings were sampled at 10 kHz and filtered at 3 kHz. For monovalent ion substitution in whole-cell experiments P_X/P_{Na} was calculated from $\exp(\Delta E_{rev}F/RT)$, and for Ca^{2+} P_{Ca}/P_{Na} was from $[Na]_i\{\exp(E_{rev}F/RT)(1 + \exp(E_{rev}F/RT)\}/4[Ca^{2+}]_o$, where $[Na]_i$ is the cytosolic Na_i concentration, F is Faraday's constant, R is the universal gas constant, T is the absolute temperature and $[Ca^{2+}]_o$ is the extracellular Ca^{2+} concentration. E_{rev} values were corrected for calculated liquid junction potentials. Numerical data are presented as means ± s.e.m.

Osmoregulation assay and contractile vacuole voiding

Wild-type and mutant AX4 strain cells were maintained in HL5 growth medium at 22 °C. Cells adherent to glass coverslips were imaged with an inverted Olympus IX71 microscope (40× objective, 1.6 numerical aperture); images were captured at 2-min intervals with Simple PCI software (C-Imaging Systems). Geometric cell size was measured offline for ten cells per field over three independent experiments. Contractile vacuoles were observed at 1-s intervals for 15 min after exposure to water, and voiding time was measured directly.

Immunoblotting and immunostaining

We used 50 μg of total cell lysate per load for perfluoro-octanoic acid PAGE19 (8%) and SDS–PAGE (4–12% gradient; NuPAGE; Invitrogen) gels. For co-localization of *Dd*P2X–GFP and calmodulin, methanol-fixed *D. discoideum* cells were permeabilized with 0.1% Triton X-100 and blocked with 3% bovine serum albumin. Cells were incubated for 1 h at room temperature with mouse monoclonal anti-calmodulin primary antibody (1:20 dilution; Sigma), washed and subsequently incubated with Cy3-conjugated donkey anti-mouse secondary antibody (Jackson Laboratories). For localization of *Dd*P2X-His in HEK 293 cells, the same protocol was performed but with anti-His tag (Invitrogen) as the primary antibody.

Generation of *Dd*P2X receptor knockout

A 3-kilobase genomic fragment encoding *Dd*P2X was amplified from wild-type AX4 genomic DNA and a tetracycline-blasticidin resistance cassette was inserted by *in vitro* transposition. This insertion is within exon 3 of the *p2xA* gene, about 650 base pairs downstream of the start codon. The linearized construct was transformed into *D. discoideum* followed by blasticidin selection. Homologous recombination was verified by polymerase chain reaction.

Acknowledgments

We thank H. Broomhead, L. Almond, K. Dossi and N. Aldren for their technical expertise during this study, and A. Mueller-Taubenberger for the gift of the pDEX 27 GFP vector. This work was supported by the Wellcome Trust, the Medical Research Council and the Lister Institute of Preventive Medicine.

References

1. North RA. Molecular physiology of P2X receptors. Physiol. Rev. 2002; 82:1013–1067. [PubMed: 12270951]
2. Khakh BS, North RA. P2X receptors as cell-surface ATP sensors in health and disease. Nature. 2006; 442:527–532. [PubMed: 16885977]
3. Gever JR, Cockayne DA, Dillon MP, Burnstock G, Ford AP. Pharmacology of P2X channels. Pflügers Arch. 2006; 452:513–537. [PubMed: 16649055]
4. Nicke A, et al. $P2X_1$ and $P2X_3$ receptors form stable trimers: a novel structural motif of ligand-gated ion channels. EMBO J. 1998; 17:3016–3028. [PubMed: 9606184]
5. Barrera NP, Ormond SJ, Henderson RM, Murrell-Lagnado RD, Edwardson JM. Atomic force microscopy imaging demonstrates that $P2X_2$ receptors are trimers but that $P2X_6$ receptor subunits do not oligomerize. J. Biol. Chem. 2005; 280:10759–10765. [PubMed: 15657042]
6. Coddou C, et al. Histidine 140 plays a key role in the inhibitory modulation of the $P2X_4$ nucleotide receptor by copper but not zinc. J. Biol. Chem. 2003; 278:36777–36785. [PubMed: 12819199]
7. Virginio C, Church D, North RA, Surprenant A. Effects of divalent cations, protons and calmidazolium at the rat $P2X_7$ receptor. Neuropharmacology. 1997; 36:1285–1294. [PubMed: 9364483]
8. Roberts JA, et al. Molecular properties of P2X receptors. Pflügers Arch. 2006; 452:486–500. [PubMed: 16607539]
9. Vial C, Roberts JA, Evans RJ. Molecular properties of ATP-gated P2X receptor ion channels. Trends Pharmacol. Sci. 2004; 25:487–493. [PubMed: 15559251]
10. Chaumont S, Jiang LH, Penna A, North RA, Rassendren F. Identification of a trafficking motif involved in the stabilization and polarization of P2X receptors. J. Biol. Chem. 2004; 279:29628–29638. [PubMed: 15126501]
11. Allen RD. The contractile vacuole and its membrane dynamics. BioEssays. 2000; 22:1035–1042. [PubMed: 11056480]
12. Zhu Q, Clarke M. Association of calmodulin and an unconventional myosin with the contractile vacuole complex of *Dictyostelium discoideum*. J. Cell Biol. 1992; 118:347–358. [PubMed: 1629238]
13. Heuser J. Evidence for recycling of contractile vacuole membrane during osmoregulation in *Dictyostelium amoebae*. Eur. J. Cell Biol. 2006; 85:859–871. [PubMed: 16831485]
14. Allen RD, Naitoh Y. Osmoregulation and contractile vacuoles of protozoa. Int. Rev. Cytol. 2002; 215:351–394. [PubMed: 11952235]
15. Gerald NJ, Sianom M, De Lozanne A. The *Dictyostelium LvsA* protein is localized on the contractile vacuole and is required for osmoregulation. Traffic. 2002; 3:50–60. [PubMed: 11872142]
16. Wu WI, Yajnik J, Siano M, De Lozanne A. Structure-function analysis of the BEACH protein LvsA. Traffic. 2004; 5:346–355. [PubMed: 15086784]
17. Jentsch TJ, Hubner CA, Fuhrmann JC. Ion channels: function unravelled by dysfunction. Nature Cell Biol. 2004; 6:1039–1047. [PubMed: 15516997]
18. Masse K, Eason R, Bhamra S, Dale N, Jones EA. Comparative genomic and expression analysis of the conserved NTPDase gene family in *Xenopus*. Genomics. 2006; 87:366–381. [PubMed: 16380227]
19. Ramjeesingh M, Huan LJ, Garami E, Bear CE. Novel method for evaluation of the oligomeric structure of membrane proteins. Biochem. J. 1999; 342:119–123. [PubMed: 10432308]

Europe PMC Funders Author Manuscripts

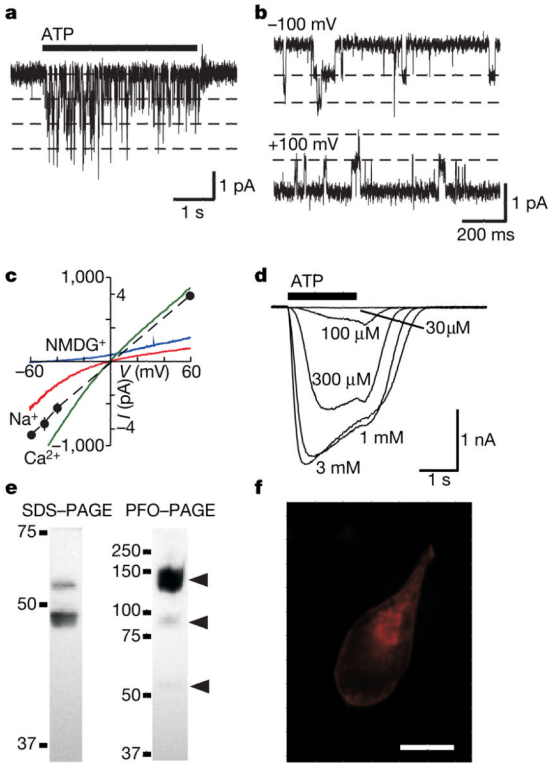

Figure 1. *Dd*P2X receptor is an ATP-gated ion channel

a, b, Single-channel openings in response to 100 μM ATP recorded from outside-out patches taken from transfected HEK 293 cells. **c**, Whole-cell current–voltage relationship shows modest inward rectification (red trace). Replacement of extracellular sodium by *N*-methyl-D-glucamine (each 147 mM) shifts reversal potential from 0 mV to −50 mV (blue trace). The current reverses close to zero with isotonic extracellular Ca^{2+} (green trace). Filled circles indicate amplitudes of unitary currents recorded in outside-out patches. Error bars indicate s.e.m. (n = 6). **d**, Concentration-dependent responses to ATP. Typical whole-cell recordings of inward currents evoked by different concentrations of ATP applied for 2 s, repeated at 2-min intervals. Cells were held at −60 mV. **e**, SDS–PAGE western blot analysis of whole-cell lysates from HEK −93 cells expressing His-tagged *Dd*P2X shows bands at 48 and 55 kDa. The mass of both bands was decreased by treatment with PNGaseF (not shown), indicating that both were *N*-glycosylated, and both bands were present at the cell surface as measured by cell-surface biotinylation. His-tagged *Dd*P2X migrates on perfluoro-octanoic acid (PFO)–PAGE predominantly as a trimer (although dimeric and monomeric species are also detectable, as indicated by the middle and lower arrows). Numbers at the left of the gels are molecular masses in kDa. **f**, Immunocytochemistry showing predominant localization of the His-tagged *Dd*P2X receptor (red; secondary antibody was Cy3) at the membrane in HEK 293 cells. Scale bar, 10 μm.

Europe PMC Funders Author Manuscripts

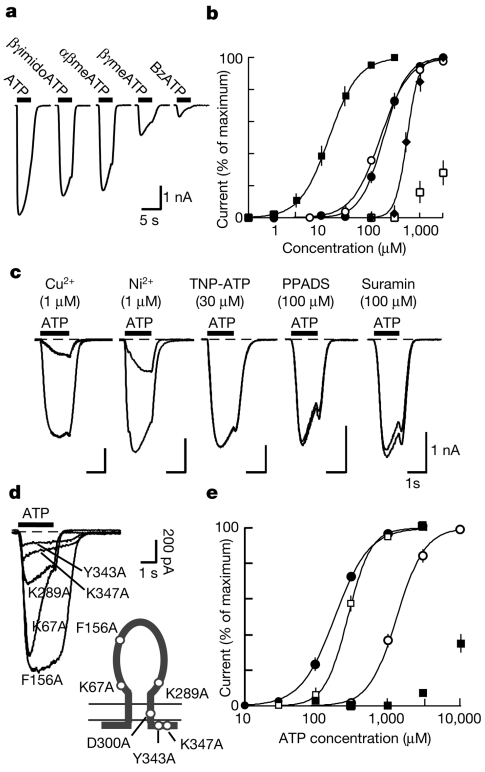

Figure 2. Properties of *Dd*P2X receptors

a, Inward currents evoked by ATP and analogues (each 300 μM, for 2 s) in HEK 293 cells expressing *Dd*P2X receptors (holding potential −60 mV). **b**, Concentration–response curves for experiments such as those shown in **a**. Responses are normalized to each maximum response and show a rank order of potency βγimidoATP (filled squares) > αβmeATP (open circles) = ATP (filled circles) > βγmeATP (filled diamonds) > benzoyl-benzyl-ATP (BzATP; open squares); each point is the mean ± s.e.m. for five to ten cells. **c**, Responses to ATP (100 μM) before and after application of Cu^{2+}, Ni^{2+} and P2X antagonists. The duration of preapplication of antagonists was 2 min (Cu^{2+} and Ni^{2+}) or 4 min (2′,3′-*O*-(2,4,6-trinitrophenyl)-adenosine 5′-triphosphate (TNP-ATP), pyridoxal-phosphate-6-azophenyl-2′, 4′-disulphonate (PPADS) and suramin). **d**, Representative whole-cell currents evoked by ATP (3 mM) in HEK 293 cells expressing mutant receptors. Lower right: diagram illustrating the topology of the P2X receptor and the relative positions of the residues mutated. **e**, Comparison of ATP sensitivity between wild-type *Dd*P2X receptors (filled circles) and the K67A (open circles), K289A (filled squares) and F156A (open squares) mutations. Each point is the mean ± s.e.m. for five to ten cells. The immunohistochemical appearance of cells expressing mutated receptors (including D330A) with the anti-His antibody was the same as that of wild-type cells. Biotinylation and SDS–PAGE followed by gel densitometry showed a highly significant expression of wild-type, K67A and D330A receptors at the cell surface.

Europe PMC Funders Author Manuscripts

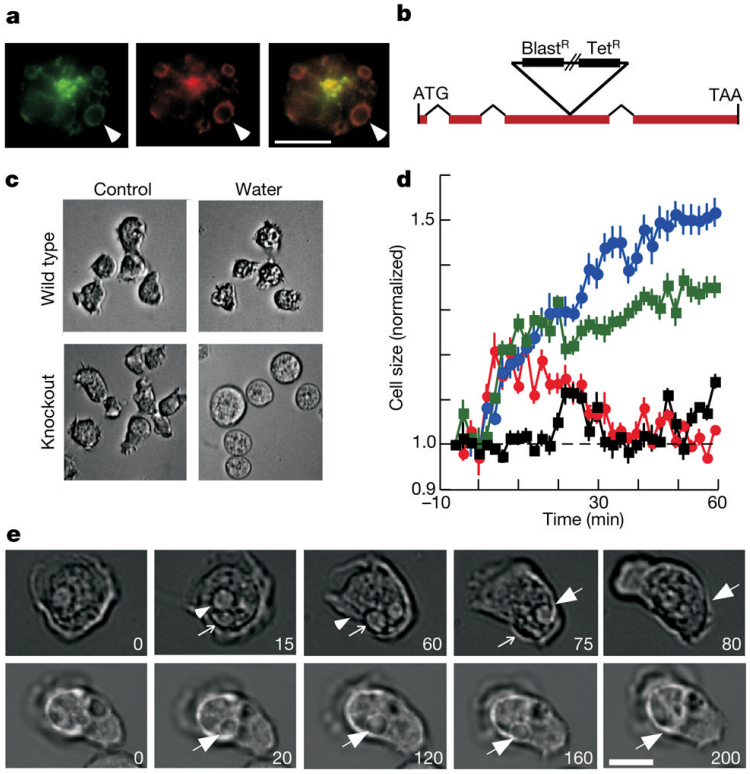

Figure 3. *Dd*P2X receptors are localized to the contractile vacuole and are required for cell volume regulation and contractile vacuole voiding

a, Co-localization of *Dd*P2X–GFP (left, green) and calmodulin (middle, red), particularly on the membrane of the contractile vacuole (arrowheads indicate one such vacuole). Right, merged image. Scale bar, 10 μm. **b**, Structure of *D. discoideum p2xA* gene to illustrate position of cassette insertion. Disruption of the *p2xA* gene caused no observable differences in cell morphology or developmental cycle (data not shown). **c**, Bright-field micrographs of *D. discoideum* in HL5 growth medium, and 60 min after change from medium to distilled water. *Dd*P2X mutant cells are swollen, whereas wild-type cells have recovered their normal volume. Scale bar, 10 μm. **d**, Time course of cell swelling and recovery. Wild-type cells (red circles) swell for 10–20 min and then regain their normal volume after about 30 min. *Dd*P2X mutant cells (blue circles) continue to swell for 60 min. Wild-type cells treated with Cu^{2+} ions (10 μM; green squares) continue to swell. Mutant cells expressing *Dd*P2X–GFP (black squares) are also similar to wild-type cells except that they show less swelling in the first 10 min. Error bars indicate s.e.m. **e**, *Dd*P2X receptors are required for normal contractile vacuole voiding. In wild-type amoebae (top row) the vacuoles (arrows) within the cell move to the membrane and void within 20–30 s. In *Dd*P2X-disrupted amoebae (bottom row) this cycle is much prolonged: the vacuole identified takes almost 3 min to discharge. Numbers indicate time in seconds. Scale bar, 5 μm.